Current Challenges for Creating a Wireless MR-Compatible Intracranial Pressure Monitor

S. Oh[1], U. Kawoos[2], M-R. Tofighi[3], A. Rosen[2], and C. M. Collins[1]

[1]Radiology, The Pennsylvania State University, Hershey, Pennsylvania, United States, [2]School of Biomedical Engineering, Drexel University, Philadelphia, Pennsylvania, United States, [3]Electrical Engineering, The Pennsylvania State University, Middletown, Pennsylvania, United States

Introduction: In the US, about 60,000 victims of traumatic brain injury (TBI) survive long enough to reach the emergency department (ED). Approximately half of these (30,000) will require careful monitoring of intracranial hypertension [1]. Besides the intracranial pressure (ICP) measurements of TBI patients in the ED, continuous ICP measurements are sometimes essential in terms of managing a patient in the intensive care unit (ICU) or in post-hospital patient care. Many studies have been focused on the accuracy and simplicity of the pressure measurements [2]. Most methods developed today include trans-cranial probes of widely varying geometry constantly being connected to a large external monitoring device. To date, they have not been designed with portability or MR compatibility in mind, although victims of TBI are among those with the greatest need for MRI. Recently, Kawoos *et al.* [3] developed a self-contained wireless device with a microelectromechanical systems (MEMS) sensor that performs the ICP measurement and can communicate results wirelessly, while being approximately the size of some existing trans-cranial probes. Wireless ICP measurement of a patient simplifies the monitoring system and could enable Telemedicine, as well as monitoring in the MR environment [4]. In this study, preliminary test results of MR compatibility (including susceptibility artifacts and temperature changes near the ICP device) in a 3.0T MRI environment are presented.

Method: Three different designs of the ICP device [3], as shown in Figure 1, were tested. First, the devices were tested to see how strongly they experienced force and torque in the MR environment. The casings of the devices were stainless steel, aluminum, and titanium for devices #1, #2, and #3, respectively. Second, general gradient-echo (GRE) and spin-echo (SE) images were acquired to observe how the device distorts the magnetic field due to magnetic susceptibility ($\chi_m/10^{-6}$cm^3/mol). A conductive agar-gel phantom (agar 7g/liter, NaCl 170mM, $CuSO_4$ 6.3mM) was prepared for temperature measurements as well as GRE and SE scanning, as shown in Figure 2(a). Each device was placed in the agar-gel phantom as depicted in Figure 2(b). Finally, temperature changes near the probe were monitored with thermo-optic probes while RF pulses with a time average power of 16.65W were delivered to the coil over a period of 2 minutes [5].

Results and Discussion: Device #1 experienced significant force and torque near the 3.0T magnet such that it could not be held stationary in a gelatin phantom, so further experiments were not performed with that device. Device #2 (Al) and device #3 (Ti) experienced very little and no discernable force, respectively. Therefore, device #2 and #3 were suitable for further testing. Significant precipitation was observed on device #2 during phantom preparation, apparently due to interaction between the aluminum casing and the copper sulfate in solution (used to shorten T_1). When the copper sulfate solution was replaced with a 1% gadolinium solution there was no precipitation. In GRE images, significant image distortions were observed near both device #2 and #3, due to the relatively large difference in magnetic susceptibility of the materials and the medium (agar-gel). The image distortions couldn't be compensated even by using SE sequence as shown in Figure 3. The magnetic susceptibilities of aluminum, titanium, and water are +16, +151, and -1.04, respectively, though the values for aluminum and titanium depend somewhat on how they are alloyed [6]. The image distortions precluded the use of MR thermography to measure temperature changes near the device during RF heating with methods demonstrated recently [5]. Therefore, the temperature changes were recorded using fiber optic thermal sensors (OpSens, Canada) near the ICP device and at a location opposite position the device (in the absence of the device, SAR and temperature change at these two locations would be identical). The temperature change rate near device #2 was 0.100°C/min compared to 0.040°C/min at the opposite location, as shown in Figure 4(a). In the view of temperature sensitivity of the ICP device (0.87mmHg/°C) [3], 0.100°C/min is high enough to affect pressure monitoring. Device #3 (of smaller diameter and titanium casing) showed a very similar temperature change rate (0.045°C/min) to the opposite location (0.040°C/min), Figure 4(b). In summary, device #3 is currently the most MR compatible, however, additional material research is required to minimize the image distortion, and additional tests with an active device are still needed.

Acknowledgment: This study was funded in part through NIH R01 EB000454 and the Pennsylvania Department of Health.

References:

[1] Marik *et al.* J Emerg Med 1999;17:711-719
[2] Sahay *et al.* J Neurosurg 1991;5:379-386
[3] Kawoos *et al.* IEEE Trans Microw Theory Tech 2008;56:2356-2365
[4] Lubecke *et al.* IEEE Microwave Magazine 2002;3:43-48
[5] Oh *et al.* 16th ISMRM 2008, Toronto, Canada, p.79
[6] Lide *et al.* "86th CRC handbook of chemistry and physics", CRC, 2006

Figure 1. ICP devices. The casing material of device #1, #2, and #3 were stainless-steel, aluminum, and titanium, respectively.

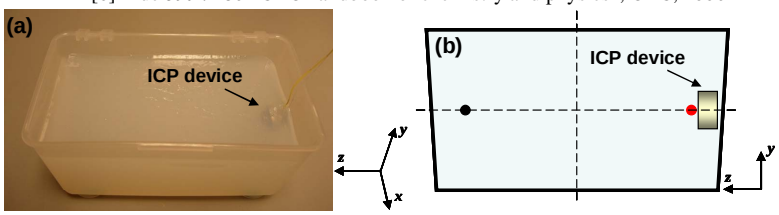

Figure 2. (a) Conductive agar-gel phantom. (width×height×depth=15×7×8.5cm^3) (b) One thermal sensor (red spot) was placed in front of the device and the other sensor (black spot) was placed at the opposite location.

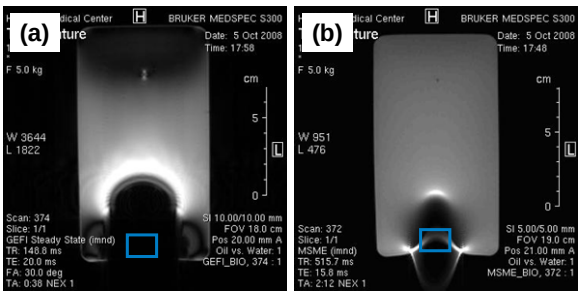

Figure 3. (a) Gradient-echo and (b) spin-echo image of device #2. Similar image distortion was observed for device #3 (not shown here). Blue rectangle indicates the position of ICP device.

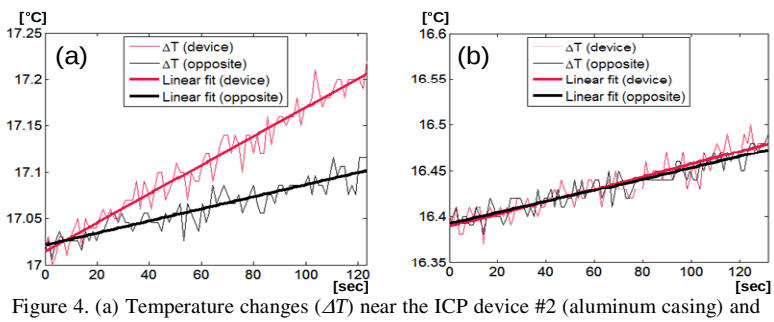

Figure 4. (a) Temperature changes (ΔT) near the ICP device #2 (aluminum casing) and (b) device #3 (titanium casing). In each figure, red and black lines correspond to red and black spots in Figure 2(b).